



# High sensitivity ICLAS of H<sub>2</sub><sup>18</sup>O in the region of the second decade (11 520–12 810 cm<sup>-1</sup>)

F. Mazzotti<sup>a</sup>, R.N. Tolchenov<sup>b</sup>, A. Campargue<sup>a,\*</sup>

<sup>a</sup> *Laboratoire de Spectrométrie Physique (associated with CNRS, UMR 5588), Université Joseph Fourier de Grenoble, B.P. 87, 38402 Saint-Martin-d'Hères Cedex, France*

<sup>b</sup> *Department of Physics and Astronomy, University College London, London WC1E 6BT, UK*

Received 13 December 2006; in revised form 23 January 2007

---

## Abstract

The high resolution absorption spectrum of the H<sub>2</sub><sup>18</sup>O isotopologue of water has been recorded by Intracavity Laser Absorption Spectroscopy (ICLAS) with a sensitivity on the order of  $\alpha_{\min} \sim 10^{-9} \text{ cm}^{-1}$ . The 11 520–12 810 cm<sup>-1</sup> spectral region corresponding to the  $3\nu + \delta$  decade of vibrational states, was explored with an ICLAS spectrometer based on a Ti:Sapphire laser. It allowed detecting transitions with an intensity down to  $10^{-27} \text{ cm/molecule}$  which is about 100 times lower than the weaker line intensities available in the literature, in particular in the HITRAN database.

The rovibrational assignment was performed on the basis of the results of variational calculations and allowed for assigning 3659 lines to the H<sub>2</sub><sup>16</sup>O, H<sub>2</sub><sup>18</sup>O, H<sub>2</sub><sup>17</sup>O, HD<sup>16</sup>O and HD<sup>18</sup>O species, leaving only 1.7% unassigned transitions. A line list including 1712 transitions of H<sub>2</sub><sup>18</sup>O has been generated and assigned leading to the determination of 692 rovibrational energy levels belonging to a total of 16 vibrational states, 386 being newly observed. A deviation on the order of 25% has been evidenced for the average intensity values given by HITRAN and the results of variational calculations. Ninety two transitions of the HD<sup>18</sup>O isotopologue could also be assigned and the corresponding upper rovibrational levels are given.

© 2007 Elsevier Inc. All rights reserved.

*Keywords:* Water; H<sub>2</sub><sup>18</sup>O; Intracavity laser absorption spectroscopy; ICLAS; Rovibrational assignment

---

## 1. Introduction

With about 0.2% abundance, H<sub>2</sub><sup>18</sup>O is the most abundant isotopologue of water after H<sub>2</sub><sup>16</sup>O. It is considered as the fifth atmospheric absorber. This is why the precise characterization of its absorption spectrum is of significant importance for atmospheric modeling, in particular in the near infrared and visible spectral regions. Most of the experimental information concerning water has been obtained by Fourier Transform Spectroscopy (FTS) which has the advantage of allowing for a wide spectral coverage and a good sensitivity when associated with long multi-pass cells. In particular, the spectroscopic parameters obtained from FTS spectra are generally those adopted in the HITRAN database [1].

In the present contribution, the weak absorption spectrum of an <sup>18</sup>O enriched sample of water has been recorded by Intracavity Laser Absorption Spectroscopy (ICLAS) in the 11 520–12 810 cm<sup>-1</sup> spectral region which covers the  $3\nu + \delta$  decade. The overview of the investigated region, as provided by different databases, is presented in Fig. 1. To our knowledge, the only absorption spectra of the H<sub>2</sub><sup>18</sup>O isotopologue available near 12 500 cm<sup>-1</sup> were obtained in the 1980s, by Chevillard et al. [2–4] at Kitt Peak National Solar Observatory. The FTS spectrometer was associated with a 6 m long White cell allowing absorption path lengths up to 434 m and the spectral resolution was 0.012 cm<sup>-1</sup>. The analysis of these spectra in our region of interest has been reported in the following contributions:

- (i) Bykov et al. [5] analyzed the 11 300–12 710 cm<sup>-1</sup> region using the effective Hamiltonian approach

---

\* Corresponding author.

E-mail address: Alain.Campargue@ujf-grenoble.fr (A. Campargue).

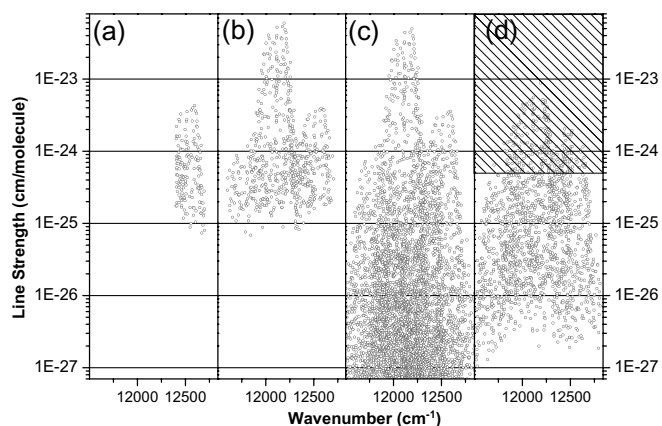


Fig. 1. Comparison of the  $\text{H}_2^{18}\text{O}$  spectrum between 11500 and 12800  $\text{cm}^{-1}$ : (a) HITRAN database [1], (b) FTS spectrum recorded at Kitt Peak [5], (c) Results of Schwenke and Partridge calculations [19,20], (d) ICLAS (this work). The dashed region corresponds to relatively strong line intensities which are saturated on the ICLAS spectra and cannot be used for line intensity retrieval. The intensity cut off was fixed to a value of  $5 \times 10^{-25}$   $\text{cm}/\text{molecule}$ . All the intensities correspond to pure  $\text{H}_2^{18}\text{O}$ .

and could determine 315 energy levels from the observation of 765 transitions reaching the (131), (211), (013), (230), (310) and (112) vibrational states

- (ii) More recently, Tanaka et al. [6,7] reanalyzed these spectra in the 12400–14520  $\text{cm}^{-1}$  region and could assign additional transitions by using recent results of variational calculations. Note that the line list attached to Ref. [7] is the one adopted in the 2004 version of the HITRAN database [1].

Laser-based techniques successfully compete with FTS associated with long multipass cells, in detecting weak transitions. In the case of less abundant isotopologues, techniques such as ICLAS or Cavity Ring Down Spectroscopy (CRDS), have the additional advantage of requiring a very small quantity of gas (typically  $10^{-3}$  mol). For instance, the spectrum of  $\text{H}_2^{18}\text{O}$  in the region of the  $5\nu$  polyad has been recorded by pulsed CRDS spectrometer with sensitivity on the order of  $2 \times 10^{-26}$   $\text{cm}/\text{molecule}$  [8]. The 11000–14000  $\text{cm}^{-1}$  region is easily accessible by using a Ti: Sapphire laser and ICLAS investigations of a large variety of molecules have been reported in this range [9]. For instance, ICLAS-Ti:Sa was applied to the study of deuterated water with a detection scheme based either on a grating spectrograph [10] or a FTS spectrometer [11,12]. We have recently reported [13] the detection of weak lines of the water main isotopologue near 12000  $\text{cm}^{-1}$  with a sensitivity as low as  $10^{-27}$   $\text{cm}/\text{molecule}$  *i.e.* at least one order of magnitude beyond the performances of the best FTS experiments [1,14–16]. In the case of  $\text{H}_2^{18}\text{O}$ , a two orders of magnitude gain in sensitivity is expected as the weakest lines detected in the Kitt Peak spectra have intensity on the order of  $10^{-25}$   $\text{cm}/\text{molecule}$  (see Fig. 1).

## 2. Experiment and line list construction

Our ICLAS spectrometer has been previously described in Refs. [9,17,18] and very recently in our work devoted to  $\text{H}_2^{16}\text{O}$  in the same spectral region [13]. The spectra were recorded with a generation time ranging between 50 and 150  $\mu\text{s}$  corresponding to an equivalent absorption path length of 4.8 and 14.4 km, respectively, as the filling ratio of the laser cavity by the absorption cell is 32%. In order to minimize the contribution of the intracavity atmospheric absorption (mainly due to  $\text{H}_2^{16}\text{O}$ ), the laser was placed in a box filled with dry nitrogen. The experimental procedure consisted in successively filling the cell with water, recording the spectrum, vacuuming the cell and recording the background spectrum. Typically, a few seconds of averaging were necessary to record a spectral window, owing to the frequency multiplex advantage of ICLAS when used with a dispersion spectrometer. The algebraic division of the spectrum by the background spectrum is a very efficient method to suppress stable spectral features frequently present in the ICLAS spectra and to increase of the signal to noise ratio. In particular, fringes due to Fabry–Perot type interferences between the fixed optical elements in the laser cavity, are totally removed by this procedure.

The grating spectrograph (79 grooves/mm) works in a high order of diffraction (about 30) allowing for a practical spectral resolution close to the doppler line width ( $0.015$   $\text{cm}^{-1}$  (HWHM) at  $12000$   $\text{cm}^{-1}$ ). The region simultaneously recorded with our 3754 diodes silicon array is about  $14$   $\text{cm}^{-1}$  wide according to the dispersion of the grating spectrograph. The wavenumber calibration of each individual spectrum requires the correction of the non linear dispersion of the grating spectrograph by using the equidistant frequency comb provided by an intracavity étalon and the use of reference lines to calibrate accurately the wavenumber scale. As we will see below, the proportion of  $\text{H}_2^{16}\text{O}$  and  $\text{H}_2^{18}\text{O}$  molecules in our sample was about 45 and 55%, respectively so that the observed spectrum exhibits many transitions of the main water isotopologue which were adopted as reference lines. The corresponding  $\text{H}_2^{16}\text{O}$  line positions were taken in the most complete set available in the literature. It resulted in using the line lists attached to Ref. [16] and Ref. [15] for the 11520–12350  $\text{cm}^{-1}$  and 12350–12780  $\text{cm}^{-1}$  spectral regions, respectively. The estimated experimental accuracy concerning the wavenumber calibration was about  $0.003$   $\text{cm}^{-1}$ , which is smaller than the frequency binning of the recording CCD array.

The  $1300$   $\text{cm}^{-1}$  wide spectral section presently investigated was covered by a total of 140 spectral snapshots. The window overlap was about  $4$   $\text{cm}^{-1}$  on each side. A series of measurements with pressures ranging between 1 and 20 Torr was recorded in order to measure weaker lines at high pressure and well resolved stronger lines at low pressure.

### Relative intensity of the $H_2^{18}O$ transitions

For each  $14\text{ cm}^{-1}$  wide spectral window, a related file was created containing a list of the line centers and the corresponding transition relative intensities. Considering the number of lines which were frequently overlapped (it was found that about 5% of the lines strongly overlapped in our final line list.), the line intensity determination was difficult and time consuming. The typical pressure broadening ( $0.0025\text{ cm}^{-1}$  (HWHM) at 20 Torr) is much smaller than the Doppler broadening ( $0.017\text{ cm}^{-1}$  (HWHM)). A gaussian function was then adopted as approximate line profile. Isolated lines were fitted by the help of a homemade software which saved the line centre as well as the integrated absorbance obtained from the fit. In the case of strong and less strong overlapping lines, the integrated absorbance (or line strength) was estimated from the absorbance value at the line centre and the average line width value of the well isolated nearby lines. Finally in case of weak overlapping lines, a multi-gaussian fit was performed.

### Absolute intensity of the $H_2^{18}O$ transitions

ICLAS is a quantitative method which provides accurate absolute intensity values [9]. However, as a result of a relatively large uncertainty on our pressure values, we decided to obtain absolute intensity values simply by scaling the relative line strengths obtained as described above, to the line strength values provided by the HITRAN database. As the HITRAN database provides  $H_2^{18}O$  lines only in the  $12400\text{--}12800\text{ cm}^{-1}$  region (see Fig. 1), we could calibrate only a small part of the spectral windows against  $H_2^{18}O$  reference lines. We hence used the  $H_2^{16}O$  lines (from Refs. [15,16]) in the  $12400\text{--}12800\text{ cm}^{-1}$  region to determine the isotopic abundance ratio between the two isotopologues. The ICLAS relative intensities were then scaled versus the  $H_2^{16}O$  absolute line intensities at 296 K over the whole studied spectral region and converted into absolute intensities for pure  $H_2^{18}O$  by using the determined concentration ratio. A value of  $0.55(7)/0.45(6)$  was obtained for the  $H_2^{18}O/H_2^{16}O$  by averaging the values obtained from spectral windows allowing for an independent calibration of the  $H_2^{16}O$  and  $H_2^{18}O$  line transitions. The uncertainties in the isotopic ratio are equal to the standard deviation of the ratios obtained on different spectral windows. It was found that because of water adsorption on the sample cell walls, the isotopic ratio slightly changed from spectrum to spectrum. Note that as the stronger lines were frequently saturated in the ICLAS spectrum and as they have been previously accurately measured by FTS, we decided to pay mainly attention to the lines with intensity lower than  $5 \times 10^{-25}\text{ cm}^2/\text{molecule}$ . This maximum value is a factor of 10 larger than the typical sensitivity of the Kitt Peak spectrum (see Fig. 1). It is difficult to estimate the uncertainty of our line intensities as it depends on the accuracy of the  $H_2^{16}O$  line intensities used as references, of the determined isotopic ratio and of our relative intensities values which

are probably not fully satisfactory in the case of weak and blended lines. We cannot rule out error on the order of 100% for the intensities of the weakest lines, while in the ideal cases of well isolated lines of medium intensity, a few % accuracy is probably achieved.

### Global line list

The most complete list of 9615 lines (including all water isotopologues) was created simply by gathering all the lines measured on the 140 individual spectral windows. Many lines appear several times in this list as a consequence of the existence of overlapping regions and of several recordings of the same spectral windows at different pressures. We decided to consider as identical two lines for which the two following criterions were satisfied (i) wavenumber difference less than  $8 \times 10^{-3}\text{ cm}^{-1}$  and (ii) line strength differed by at most a factor of 2 for weak lines just above the noise level. By averaging the position and intensities of these identical lines (including all water isotopologues), the number of lines was decreased from 9615 to 3624 which is the line list considered in the forthcoming rovibrational analysis. The line list including rovibrational assignments, Schwenke and Partridge (SP) calculated positions and intensities [19,20], is attached to the paper as **Supplementary Material**. For convenience of the user, we have completed this line list with 177 stronger  $H_2^{18}O$  lines previously measured by FTS as they could not be accurately measured by ICLAS because of saturation effects. The line positions of these strong lines were taken from Ref. [5] and the corresponding SP line intensities are given.

### 3. Line assignment and energy level derivation

Five water isotopologues were found to contribute to the observed spectrum:  $H_2^{16}O$ ,  $H_2^{18}O$ ,  $H_2^{17}O$ ,  $HD^{16}O$ , and  $HD^{18}O$ . For each of these species, the assignment was based on the results of SP calculations [19,20] as available on the web-based spectroscopic information system SPECTRA of the Institute of Atmospheric Optics in Tomsk, Russia (<http://spectra.iao.ru>). The calculated intensities were scaled to match on average the corresponding experimental values. The correspondence between the experimental and calculated lines was found by using the usual criteria: agreement in frequencies and intensities, combination difference relations and smooth dependence versus the rotational quantum numbers, of the difference between the experimental energy level and SP calculated values. In a second step, the assignments to each isotopologue were checked against their known experimental levels and corrected when necessary; the major attention being given to  $H_2^{18}O$ . The previous experimental studies relevant for this checking are the followings:  $H_2^{16}O$  [13, 15 and 16],  $H_2^{18}O$  [5–7],  $H_2^{17}O$  [7] and  $HD^{16}O$  [10]. As a result, the number of lines assigned for each isotopologue is:  $H_2^{16}O$ : 1553,  $H_2^{18}O$ : 1712,  $H_2^{17}O$ : 326,  $HD^{16}O$ : 68 and  $HD^{18}O$ :

92, leaving unassigned only 61 lines (1.7%). Two examples of spectra assignment are given in Figs. 2 and 3.

The new experimental information derived from this analysis concerns the  $\text{H}_2^{18}\text{O}$  and  $\text{HD}^{18}\text{O}$  isotopologues and we will then limit the further discussion to these species. In the investigated spectral region, no transition was previously reported for the  $\text{HD}^{18}\text{O}$  isotopologue. As illustrated in Figs. 1–3, the two orders of magnitude gain in sensitivity achieved by ICLAS compared to Kitt Peak spectra allows extending importantly the knowledge of the  $\text{H}_2^{18}\text{O}$  species: over the 1712 transitions assigned to  $\text{H}_2^{18}\text{O}$ , 774 were found to reach new energy levels. It resulted in the derivation of 692 energy levels belonging to 16 vibrational states, 386 of them being newly determined. The upper level energies were derived by adding the lower energy values [21] to the observed transitions. About 47% and 18% of the predicted transitions with line strengths in the range  $2 \times 10^{-27}$ – $5 \times 10^{-25}$  and  $1 \times 10^{-26}$ – $5 \times 10^{-25}$  cm/molecule, respectively, were not observed. These percentages give an evaluation of the fraction of weak  $\text{H}_2^{18}\text{O}$  lines obscured by strong lines of  $\text{H}_2^{16}\text{O}$  or  $\text{H}_2^{17}\text{O}$ .

A state by state comparison with previous FTS analysis is presented in Table 1. The corresponding total number of levels determined by Bykov et al. [5] in the 11300–12710  $\text{cm}^{-1}$  region and Tanaka et al. [7] in the wider 12400–14520  $\text{cm}^{-1}$  region, were 315 and 365, respectively. The whole set of energy levels is listed in Tables 2–4 in which the deviations of the observed levels from their calculated values [19] are also included. These tables give the uncertainty on the energy level value when determined through different transitions. Additional information about the quality of the energy levels can be found in the energy

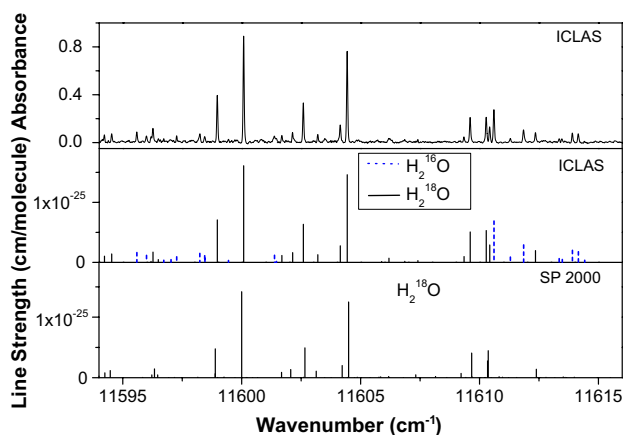


Fig. 2.  $\text{H}_2^{18}\text{O}$  spectrum in a spectral section around  $11605\text{cm}^{-1}$ : (a) ICLAS spectrum recorded with an  $^{18}\text{O}$  enriched sample of water (total pressure: 18 hPa, absorption equivalent pathlength of 14.4 km corresponding to a 150  $\mu\text{s}$  generation time). (b) Stick spectrum of the  $\text{H}_2^{16}\text{O}$  (dashed line) and  $\text{H}_2^{18}\text{O}$  (solid lines) retrieved from the ICLAS spectrum. The line intensities correspond to pure  $\text{H}_2^{18}\text{O}$  and the  $\text{H}_2^{16}\text{O}$  line intensities were scaled to best match the above ICLAS spectrum. (c) Results of Schwenke and Partridge variational calculations for  $\text{H}_2^{18}\text{O}$  [19,20]. Note that only the two strongest lines of the region were detected in Kitt Peak FTS [5].

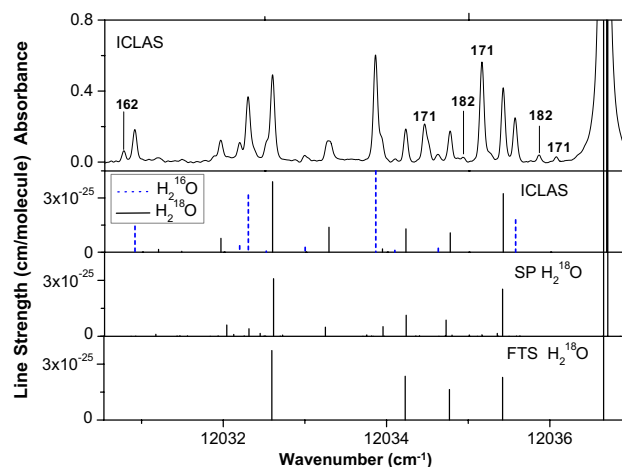


Fig. 3. Comparison of  $\text{H}_2^{18}\text{O}$  spectrum in a spectral section around  $12035\text{cm}^{-1}$ : (a) ICLAS spectrum recorded with an  $^{18}\text{O}$  enriched sample of water (total pressure 18 hPa, absorption equivalent path length of 4.8 km corresponding to a 50  $\mu\text{s}$  generation time) showing the contribution of different isotopologues. The  $\text{H}_2^{16}\text{O}$  and  $\text{H}_2^{18}\text{O}$  species are easily identified by comparison with (b) while the  $\text{H}_2^{17}\text{O}$ ,  $\text{HD}^{16}\text{O}$ , and  $\text{HD}^{18}\text{O}$  isotopologues are marked by 171, 162 and 182, respectively, (b) Stick spectrum of the  $\text{H}_2^{16}\text{O}$  and  $\text{H}_2^{18}\text{O}$  isotopologues retrieved from the ICLAS spectrum. The line intensities correspond to pure  $\text{H}_2^{18}\text{O}$  and the  $\text{H}_2^{16}\text{O}$  line intensities were scaled to match approximately the above ICLAS spectrum, (c) Results of the Schwenke and Partridge [19,20] variational calculations for  $\text{H}_2^{18}\text{O}$ , (d) Kitt Peak stick  $\text{H}_2^{18}\text{O}$  spectrum [5].

level file provided in the Supplementary Material. For each rovibrational level, three labels are given to indicate if any problematic lines were used to derive the corresponding

Table 1

Comparison of the number of energy levels determined from the vibrational bands of  $\text{H}_2^{18}\text{O}$  recorded by ICLAS between 11520 and  $12810\text{cm}^{-1}$  and the previous analysis of Kitt Peak FTS spectra [5,7]

Vibrational level	Vib. Term. <sup>a</sup> ( $\text{cm}^{-1}$ )	Number of observed levels		
		Ref. [7]	Ref. [5]	ICLAS
003	10993.680			1
013	12520.123	72	65	105
023	14015.6*	12		2
032	11963.537			64
051	11199.4*			7
061	12538.5*			1
080	11214.0*			2
090	12339.0*			1
112	12372.705	45	50	95
131	11774.707		51	102
150	11274.5*			4
160	12488.0*			1
211	12116.815		87	128
221	13612.5*	72		8
230	11734.525		10	69
310	12106.978	1	52	102
Total		202	315	692

<sup>a</sup> The vibrational term values marked by \* are those calculated by Schwenke and Partridge [19] for the  $0_{0,0}$  rotational level. The other values are experimental values presently determined (except for the value of the (003) state which is reproduced from Ref. [3]).

Table 2  
Energy levels of the (230), (131), (032) and (310) vibrational states of H<sub>2</sub><sup>18</sup>O

$JK_aK_c$	(230)				(131)				(032)				(310)			
	$E_{\text{obs}}$ (cm <sup>-1</sup> )	$\sigma$	$N$	$\Delta$	$E_{\text{obs}}$ (cm <sup>-1</sup> )	$\sigma$	$N$	$\Delta$	$E_{\text{obs}}$ (cm <sup>-1</sup> )	$\sigma$	$N$	$\Delta$	$E_{\text{obs}}$ (cm <sup>-1</sup> )	$\sigma$	$N$	$\Delta$
000	11734.5250		1	-100	11774.7067		1	33	11963.5372		1	-77	12106.9776		1	-28
101	11757.5444		1	-95	11797.9134	0.7	2	40	11986.9193		1	-77	12129.7423		1	-18
111	11781.1470	2.1	2	-92	11820.0649		1	42	12008.0046		1	-78	12143.4722	1.6	3	-25
110	11787.2915	0.6	2	-91	11826.2574	1.9	2	24	12014.2761	2.5	2	-80	12148.8514	1.1	2	-21
202	11802.4850	0.2	2	-95	11843.1421	2.2	2	42	12032.4360		1	-77	12173.8481		1	-26
212	11821.0773	1.2	3	-88	11860.2638	0.5	3	42	12048.5290	2.2	3	-74	12182.3718	0.6	2	-26
211	11839.4607	1.4	3	-87	11878.7945	0.3	3	21	12067.3082		1	-78	12199.8482	2.0	2	-17
221	11907.6526	0.5	4	-82	11943.4263	0.7	2	40	12128.8570	0.7	2	-64	12240.3412	1.7	2	-28
220	11908.6823		1	-74	11944.5510		2	40					12241.6729		1	-19
303	11867.4124	0.8	2	-91	11908.3252	7.4	2	18	12097.9170	0.0	2	-74	12237.0421	4.0	3	-11
313	11880.3344	0.5	3	-92	11919.8856	0.3	2	44					12242.1141	1.5	3	-30
312	11916.8492*	0.1	2	-85	11956.6456	1.2	3	42	12145.8749	0.9	2	-71	12275.2578	3.1	2	-5
322	11976.9670	0.2	2	-64	12013.1143	0.9	2	46	12199.1587	0.6	2	-74	12308.7365	1.2	3	-13
321	11981.8795	0.6	4	-69	12018.4578	1.9	2	24	12204.8414	1.9	3	-76	12314.9049	1.3	4	-9
331	12100.3934		1	-62	12131.6774	1.3	3	35	12313.2082		1	-68	12389.3307		1	-9
330	12100.5457	0.9	3	-56	12131.8089	0.3	2	35	12313.3584		1	-83	12389.5364	0.1	2	-7
404	11950.2671*		1	-82	11991.3860		1	55	12181.2242	0.5	2	-70	12317.4386	0.9	2	-12
414	11958.3165*	0.8	3	-73	11998.3053	0.9	3	50	12187.2535	3.4	2	-76	12319.8877	0.6	3	-13
413	12018.3083	0.1	2	-87	12058.4330	1.2	4	40	12248.6140		1	-63	12373.5062	2.0	3	-13
423	12068.5898*	0.7	3	-50	12105.0025	2.9	3	20	12291.7524	1.3	3	-71	12398.8016	1.3	5	-5
422	12081.9985	2.4	2	-63	12119.6118	1.1	3	52	12307.1822		1	-62	12414.9323	1.0	4	1
432	12195.0479	0.5	4	-43	12226.6838	1.6	4	42	12409.2437	2.4	3	-80	12482.7504	2.0	2	2
431	12195.6045		1	-57	12227.5749	0.2	3	41	12410.2696		1	-64	12484.1666	2.4	4	-12
441	12355.5552	0.6	2	-32	12381.1870		1	5	12557.7220		1	-71	12590.5827	1.4	3	1
440	12355.5804		1	-33	12381.2114		1	26	12557.7387		1	-71	12590.6088		1	-13
505	12049.7801	0.7	3	-67	12091.0938	1.2	3	35	12281.2372	0.9	2	-64	12414.4453	2.2	3	-6
515	12054.4498		1	-72	12094.9037	0.9	2	55	12284.4617		1	-50	12415.5190	2.4	2	-17
514	12142.1490	0.5	3	-66	12184.5080*	1.3	3	53	12373.5929	1.2	3	-57	12492.3335	4.8	3	3
524	12179.6363	2.9	2	-39	12218.3625	0.6	4	51					12509.8594	0.3	4	6
523	12209.3119	0.2	2	-61	12248.1364*	3.5	4	31	12437.0527	8.8	2	-72	12541.1461	2.0	4	6
533	12312.8147	2.5	2	-45	12345.2845	1.0	4	43	12529.1357		1	-56	12599.2993	1.2	4	-4
532	12315.5846	0.9	4	-42	12348.6574	0.9	3	44	12532.9207		1	-74	12604.4635	2.6	2	10
542	12474.0947	2.3	3	-16	12500.1603	0.7	5	27					12707.9663	0.8	2	6
541	12474.3001	1.8	3	-19	12500.3789	0.3	3	6	12677.2482	0.8	2	-64	12708.2345	0.8	2	6
551					12687.7762		1	18	12859.5917		1	-114	12840.7543		1	63
550	12667.5444		1	-3	12687.7377	22.3	2	-6	12859.6355	1.8	2	-133	12840.7831		1	81
606	12165.6013	2.9	2	-58	12207.2096	1.3	2	62	12397.8354		1	-66	12528.2089		1	0
616	12168.2798	0.7	2	-51	12209.2569	1.4	2	57	12398.7840	0.3	2	-57	12528.6561		1	-3
615	12286.2147		1	-53	12327.8973	0.9	3	74					12629.2578	1.1	2	14
625	12314.0449	1.0	4	-42	12352.4397*		1	65	12540.2967		1	-64	12636.5418	0.9	4	3
624	12362.8531	2.7	3	-57	12403.5162	0.9	3	53					12691.8711		1	19
634	12453.6053		1	-26	12486.9549*	0.9	4	46	12672.3405	1.5	2	-64	12738.3202	0.7	3	15
633	12461.4774	3.8	2	-33	12496.1710	0.4	4	50					12751.6323	2.4	2	24
643	12616.0833		1	-9	12641.9333	0.9	4	24	12820.6292	0.9	3	-63	12849.1013*	3.3	3	13
642					12643.7077	1.2	3	30	12821.2603		1	-62	12850.2561	1.0	2	11
652	12810.3613	0.2	2	15	12831.8036	4.4	2	41	13005.0665	0.7	4	-45	12981.5745		1	88
651					12831.7117	3.2	2	44					12981.7966		1	93
661					13042.8409		1	5	13209.1990		1	-99	13145.9954		1	153
660					13042.8467		1	10	13209.2157	14.4	2	-82	13145.9330		1	151
707	12297.8729	2.6	2	-46	12339.8791	0.1	2	66	12529.9024		1	-68				
717	12299.5297		1	-43	12341.0752	1.1	3	67	12531.5042		1	-58	12659.1459		1	-8
716	12448.3318	1.2	2	-34	12489.9225	0.6	2	84	12680.6802		1	-54	12782.6117		1	26
726	12467.7635	9.9	2	3	12506.9445	1.8	3	77	12694.1789		1	-48	12788.3338	0.4	2	20
725	12542.2745		1	-28	12582.3595	1.2	3	73	12772.3856		1	-55	12864.7974	0.6	2	32
735	12616.6291	4.3	2	-3	12650.4771	1.6	4	41					12898.8393	1.4	3	24
734	12634.0467		1	-32	12670.8410		1	47	12859.8783		1	-62	12925.8291*	1.2	2	40
744	12779.9772		1	-2	12811.6574	2.3	5	37	12987.8603	1.5	2	-56	13013.2940	0.9	2	99
743	12785.0786	3.7	3	16	12811.5067	1.2	2	29	12989.6870	3.2	2	-60	13017.805	2.7	4	65
753					12999.8777	1.3	2	47					13145.5457	1.6	2	99
752	12976.9858		1	22	12999.3658	2.0	2	55	13172.0896	4.2	2	-112	13146.4573*		1	107
762					13210.8123	0.8	3	3					13311.7418		1	179
761					13210.8224	16.8	2	22					13312.4085		1	133

Table 2 (continued)

$JK_aK_c$	(230)				(131)				(032)				(310)			
	$E_{\text{obs}} (\text{cm}^{-1})$	$\sigma$	$N$	$\Delta$	$E_{\text{obs}} (\text{cm}^{-1})$	$\sigma$	$N$	$\Delta$	$E_{\text{obs}} (\text{cm}^{-1})$	$\sigma$	$N$	$\Delta$	$E_{\text{obs}} (\text{cm}^{-1})$	$\sigma$	$N$	$\Delta$
770									13604.5321		1	-36	13437.1810		1	257
808	12446.9919		1	-32	12489.3172		1	77					12806.3779		1	-9
818	12448.1633	3.5	2	-23	12490.4034	0.8	2	80					12808.0558		1	-4
817	12626.9563	8.3	2	-28	12668.4974	0.9	3	84					12952.0877		1	124
827	12641.5210	0.1	2	31					12865.4547		1	-44	12952.6148	0.2	2	16
826	12742.5132		1	-58	12783.3694	0.2	4	68					13056.9875		1	32
836	12799.8827		1	5	12837.7298	2.5	2	41					13081.6550	0.8	5	42
835					12874.3217	0.6	3	52					13125.6560	0.8	3	52
845	12973.5317	1.5	2	16	13001.5305	0.1	2	40	13178.5014		1	-59	13201.0502		1	48
844					13004.1845	1.3	3	23	13192.6441	3.7	2	50	13211.7693		1	102
854	13166.7002		1	45	13182.6206		1	-32					13331.9172		1	85
853					13190.3297		1	70								
863					13402.3285	0.3	2	0	13570.5118		1	-106	13501.0595		1	201
862					13402.2562		1	1					13501.7761		1	175
872	13709.3012		1	408					13798.7141		1	-45	13938.9548		1	189
871					13710.3773		1	280								
881													14045.2336		1	410
880					13792.5572		1	-221								
909					12655.7461	1.8	2	80					12972.4938	0.6	2	-9
919					12660.2612		1	95					12970.2791		1	-11
918	12821.4954		1	-6	12863.3858		1	107	13049.8335	4.6	2	-75	13137.8108		1	31
928					12863.6025	3.3	2	60								
927	12962.1370		1	-21	13010.0686		1	76					13267.8167		1	47
937	13002.7670		1	-502	13043.4827	0.3	2	54	13232.4397		1	13	13275.2832	0.6	3	24
936					13100.4850		1	57					13348.5340	4.2	2	50
946					13214.5020		1	42	13409.6887		1	59	13413.6417		1	92
945	13187.2280		1	-41	13221.3552		1	-3	13411.7184		1	35	13432.0821		1	56
955					13398.8506		1	-11								
954					13401.3779		1	49					13547.6252		1	119
964					13616.5652		1	3								
963	13553.4872		1	119	13617.0494		1	-4								
973					13926.1148		1	159								
972													13843.1461		1	298
982					14005.9484		1	-243								
10010					12839.9709		1	91					13417.7731		1	19
10110													13152.0965		1	-19
1019					13076.2652		1	130					13339.6632		1	-116
1029					13072.5030		1	64					13337.3548	1.1	3	29
1028					13246.4070		1	102								
1038									13456.8546		1	-60	13499.0790	1.2	2	24
1047									13648.3722	1.6	2	81	13641.3974		1	88
1046					13470.2890		1	43								
1056													13784.5277		1	135
1055													13785.0728		1	116
1065													13949.6191		1	246
1074																
11011													13350.6102		1	-43
11111					13036.8706		1	73								
11210					13298.1974		1	88								
11210					13298.1974		1	88								
1129													13736.1928		1	61
1139													13727.0218		1	4
1138	13576.5609		1	12												
1148					13705.5870		1	10	13897.0961		1	43				
1156													14322.9226		1	137
1165													14471.5433		1	149
1175					14426.6719		1	63								
12012					13253.1916		1	82								
12310									13965.5951		1	-94	14255.6363		1	58
1248					14047.9220		1	85								
1258													14316.5803		1	110

Note.  $N$  is the number of lines used for the upper energy level determination,  $\sigma$  denotes the corresponding standard deviation calculated for energies determined from more than one transition in  $10^{-3} \text{ cm}^{-1}$  units and  $\Delta$  is the deviation of the observed levels from their calculated [19] values in  $10^{-3} \text{ cm}^{-1}$ . Levels marked by \* are in disagreement with those reported in Ref. [5].

Table 3  
Energy levels of the (211), (112) and (013) vibrational states of H<sub>2</sub><sup>18</sup>O

$JK_aK_c$	(211)				(112)				(013)			
	$E_{\text{obs.}} (\text{cm}^{-1})$	$\sigma$	$N$	$\Delta$	$E_{\text{obs.}} (\text{cm}^{-1})$	$\sigma$	$N$	$\Delta$	$E_{\text{obs.}} (\text{cm}^{-1})$	$\sigma$	$N$	$\Delta$
000	12116.8148		1	-21	12372.7045		1	42	12520.1234		1	56
101	12139.4429				12395.5226	0.1	2	46	12543.2309	0.0	2	63
111	12152.9458		1	-33	12408.7973	0.9	3	41	12555.3766	2.7	2	69
110	12158.5055				12414.3831		1	43	12561.0828		1	72
202	12184.6750		1	-24	12439.7095	1.0	2	46	12587.8106		1	58
212	12192.9163		1	-34	12448.8445	0.6	3	43	12595.8891	0.4	2	64
211	12209.5335		1	-50	12465.5716	0.4	3	46	12612.9928		1	80
221	12249.3643	0.8	2	-27	12505.3433	1.1	3	36	12649.0258	1.2	2	66
220	12250.7607	3.7	2	-33	12506.7552	0.7	2	53	12650.6133	1.3	2	64
303	12247.2810	1.4	2	-38	12502.9510	0.5	3	47	12651.1968	0.3	2	73
313	12252.1098	0.7	3	-28	12508.0806	0.7	2	30	12655.7295	1.7	2	63
312	12284.9474	0.5	3	-19	12541.2109	0.0	2	47	12689.5440	0.0	2	67
322	12317.6522	1.4	2	-22	12573.7974	0.5	5	52	12718.4472	0.8	3	67
321	12324.1128	0.8	5	-33	12580.2840	3.5	3	48	12725.6516	0.6	4	81
331	12397.4688	4.0	2	-15	12653.6167	1.4	4	45	12792.3556	0.1	4	68
330	12397.6976		1	-18	12653.6739	0.7	4	59	12792.6474	1.1	2	66
404	12327.5791	0.1	2	-21	12583.5143	0.7	2	31	12731.9896		1	62
414	12329.8604	0.7	2	-23	12585.8110	1.1	4	46	12734.1433		1	48
413	12383.0613	3.0	2	-9	12639.6848	0.9	3	38	12788.8539	1.4	3	70
423	12407.5054		1	-30	12663.8254	6.0	5	50	12809.5788		1	84
422	12424.3363	1.4	4	-9	12680.7516	0.9	5	57	12828.0034		1	65
432	12490.8327	0.7	3	-12	12747.1377	1.1	4	61	12887.7532	0.9	4	71
431	12492.3687	0.2	3	-9	12748.5089	1.3	5	49	12889.6457	0.8	3	71
441	12597.3561	0.9	2	-13	12852.8830	3.0	4	73	12985.1955	0.6	2	82
440	12597.3864	0.9	3	-2	12852.8797	1.8	3	70	12985.2438	0.9	3	71
505	12424.6186	0.9	2	-36	12680.0950		2	-1	12829.5228	0.9	3	71
515	12425.5860	0.4	2	-20	12681.4688		1	34	12830.6608		1	58
514	12501.3453		2	-5	12758.6394	1.5	4	59	12908.2655	0.5	3	70
524	12518.1262	0.9	2	-7	12774.5020	0.8	4	61	12921.3754	0.5	3	67
523	12550.7400	1.2	3	-16	12807.3394	0.9	4	62	12956.6192	0.8	3	87
533	12607.3117	1.0	4	-3	12864.1157	1.4	4	52	13006.5679	1.0	3	75
532	12612.8595	1.6	6	2	12869.3372	1.2	5	64	13013.1672	0.9	4	68
542	12714.5646	0.3	3	7	12970.1885	0.1	2	76	13108.8782	7.1	4	81
541	12714.8399	1.1	3	-13	12970.2579	1.7	4	73	13109.1026	2.2	2	93
551	12848.2381		1	28	13098.8304	0.3	2	70	13225.9351		1	59
550	12848.2412		1	31	13098.6631	0.5	3	75	13225.9507		1	69
606	12538.4747	2.4	2	-19	12794.0514		1	41	12944.0103	0.4	2	56
616	12538.9016	0.4	2	-20	12794.6744	0.1	3	50	12943.9995	0.6	3	52
615	12641.8862	0.5	3	12	12895.5801	0.5	3	64	13045.2393	0.6	4	67
625	12649.5880	0.3	3	7	12904.8393	0.7	4	67	13052.8860	0.5	3	69
624	12701.5408	1.3	5	10	12959.1435	0.9	3	66	13109.3285		1	53
634	12746.2170	0.6	5	3	13002.5358	1.5	4	-5	13148.0772	2.9	2	79
633	12760.3973	2.2	5	16	13017.2924	0.9	4	71	13164.3591	1.7	4	76
643	12855.4210	0.6	4	21	13111.2771	0.8	4	81	13253.6598	1.3	3	99
642	12856.6935	1.6	6	19	13111.9185		1	74	13254.7144	8.3	3	92
652	12989.2226	1.6	2	35	13239.2470	0.1	2	72	13368.0645		1	70
651	12989.2621	0.5	3	48	13238.5876	0.4	2	74	13368.1289*	0.1	2	72
661	13151.2170		1	98	13402.5737		1	125				
660	13151.2185		1	92					13512.4530*		1	76
707	12669.3197		1	-21	12924.9560	8.0	2	61	13075.6053	0.0	2	45
717	12669.7741	0.2	2	-14	12925.3279	1.6	2	49	13075.6737		1	45
716	12794.1463		1	12	13048.9659	0.2	3	69	13198.5454	0.7	4	61
726	12795.7346	0.7	4	5	13054.0234	0.8	3	72	13204.4582	0.1	2	75
725	12874.3542	2.5	3	17	13132.2504	1.4	4	31	13283.4531	0.8	2	67
735	12906.5845		1	13	13164.6163	1.8	3	73	13310.4632*	1.9	4	96
734	12935.0374	1.1	4	32	13191.1224	0.5	2	68	13342.8092	1.4	3	76
744	13019.6535	0.6	4	34	13275.7826		1	90	13421.6602	1.1	2	102
743	13023.7989	0.7	4	29	13278.5654	1.1	3	78	13425.3618		1	93

Note.  $N$  is the number of lines used for the upper energy level determination,  $\sigma$  denotes the corresponding standard deviation calculated for energies determined from more than one transition in  $10^{-3} \text{ cm}^{-1}$  units and  $\Delta$  is the deviation of the observed levels from their calculated values [19] in  $10^{-3} \text{ cm}^{-1}$ . Levels marked by \* and + are in disagreement with those reported in Ref. [5] and Ref. [7], respectively. For completeness, the energy values of the [101] and [110] levels of the (211) vibrational state are reproduced from Ref. [5] as the corresponding transitions are saturated in the ICLAS spectrum.

Table 3 (continued)

$JK_aK_c$	(211)				(112)				(013)			
	$E_{\text{obs}}$ (cm <sup>-1</sup> )	$\sigma$	$N$	$\Delta$	$E_{\text{obs}}$ (cm <sup>-1</sup> )	$\sigma$	$N$	$\Delta$	$E_{\text{obs}}$ (cm <sup>-1</sup> )	$\sigma$	$N$	$\Delta$
753	13153.8514	0.8	2	54	13404.3509		1	80				
752	13154.0374	2.3	5	66	13402.6550	4.4	2	82	13534.3497		1	69
762	13316.6740		1	122	13569.4223		1	160	13679.0913	0.1	2	80
761	13316.6793	7.1	2	110	13569.3840		1	122				
771	13437.1064	1.0	2	-2								
770	13437.1078		1	-1	13748.6055		1	175				
808	12817.5826		1	-17	13072.9422*	2.8	2	49	13224.4051	2.5	3	40
818	12816.5635		1	-27	13071.7020*		1	25	13224.3890		1	32
817	12961.8256	1.3	3	14	13218.6478	0.1	2	73	13368.1674	0.2	3	52
827	12963.2691	0.9	4	8	13221.7287	2.1	4	77	13368.8053*	1.4	3	47
826	13066.4118	0.8	3	27	13324.4956		1	80	13476.0040	0.3	3	59
836	13087.7043	0.9	2	14	13347.6871*	0.8	4	92	13494.7185		1	77
835	13135.2579	0.4	2	47	13396.0062	0.2	2	91	13546.6099		1	47
845	13206.5792	1.4	3	44	13463.0104	1.9	3	93	13612.6676		1	99
844	13217.2436	2.7	4	37	13470.6823		1	70	13622.6055		1	83
854	13342.0742	0.7	2	71					13723.6345		1	49
853	13342.7903	0.4	3	82	13590.5856		1	76	13724.9210	0.1	2	68
863	13505.6176		1	141	13759.8859		1	144				
862	13505.6701	0.9	3	128	13759.7863		1	140	13869.5479		1	64
871	13628.1983	0.5	3	-9					14032.5553		1	91
880									14213.5941		1	85
909	12981.1403	1.3	3	-25	13237.0279		1	31	13390.2746		1	25
919	12981.8952	1.1	3	-30	13239.2860*		1	8	13390.2799		1	23
918	13147.9845	0.5	4	18	13404.0812	1.0	3	70	13553.6585		1	60
928	13148.1141	0.1	2	17					13554.7772		1	45
927	13282.5249	1.7	2	40	13533.8363		1	76	13684.8437		1	52
937	13288.0590	2.9	4	17	13538.1441	2.7	2	63	13701.5649		1	95
936	13358.4250	1.5	3	58	13621.0636	1.2	2	80	13773.4009		1	88
946	13416.4575	1.2	4	60	13672.1061	1.5	2	89	13826.2871		1	107
945	13437.8607	1.6	3	53	13685.3778		1	47	13847.6668		1	88
955	13553.6063	1.0	3	77	13806.3401		1	99	13936.6731		1	49
954	13556.7241	2.9	3	88	13802.2726		1	69				
964	13717.9544	1.3	2	161	13974.1618		1	159	14084.0041		1	54
963					13973.6923		1	144				
973	13842.3564	4.6	2	-22								
972					14152.5285		1	203				
10010	13163.2881		1	-56					13573.3523		1	-6
10110	13163.2545		1	-60	13418.2785		1	34	13573.3881		1	26
1019	13346.0860	1.7	3	28					13757.3077	6.5	2	47
1029	13349.5964	2.5	3	37	13604.8239	0.4	2	72	13757.5682		1	37
1028	13505.1904	0.2	2	27					13909.2421		1	27
1038	13507.2730		1	-4	13760.2684		1	-84	13911.6000		1	19
1037	13600.5358	0.0	3	38					14019.6143		1	76
1047	13646.4968		1	51	13902.1375	4.5	2	86				
1046	13684.9107	1.3	3	52					14099.1813		1	61
1056					14041.5060		1	104				
1055	13794.5063	1.4	3	108								
1065	13953.3780		1	60	14212.7225		1	154				
1064	13954.0127	2.5	2	156								
1073	14079.3817		1	-28								
11011	13362.0990	2.0	2	-55	13617.0849		1	25	13773.7005+		1	-6
11111	13362.0980	3.6	2	-63					13773.5158		1	-17
11210	13567.1425		1	27					13977.4415		1	20
1129	13740.0941		1	17	14000.1303		1	72	14149.4297		1	6
1139	13745.1607		1	-4					14150.9266		1	-1
1138	13862.7517		1	49					14282.6669		1	57
1148	13897.1372		1	42								
1147	13957.1900		1	40								
12012	13577.7683		1	-69					13991.1324		1	-32
12112	13577.7692		1	-53					13989.8851		1	-47
12111	13804.2716	0.8	2	-1					14215.5582		1	71
12211	13804.2404		1	-1								
12210	13997.9066	6.9	3	8					14406.1591		1	-13

(continued on next page)

Table 3 (continued)

$JK_aK_c$	(211)				(112)				(013)			
	$E_{\text{obs}}$ (cm <sup>-1</sup> )	$\sigma$	$N$	$\Delta$	$E_{\text{obs}}$ (cm <sup>-1</sup> )	$\sigma$	$N$	$\Delta$	$E_{\text{obs}}$ (cm <sup>-1</sup> )	$\sigma$	$N$	$\Delta$
12310	13998.7880		1	4								
1239	14140.4631		1	37								
1248	14249.0715		1	35								
1257	14349.3577		1	109								
13013	13810.2766		1	-144								
13113	13810.2767	0.3	2	-142					14223.8492		1	-110
13112	14057.0729		1	-60								
13212	14057.0930		1	-8					14469.1323		1	0
13211	14271.0121		1	-4								
13311	14270.3987		1	-11								
13410	14452.1982		1	76								
14014	14062.4019		1	71								

Table 4

Energy levels of the (003), (023), (051), (061), (080), (090), (150), (160) and (221) vibrational states of H<sub>2</sub><sup>18</sup>O

$JK_aK_c$	$E_{\text{obs}}$ (cm <sup>-1</sup> )	$\sigma$	$N$	$\Delta$
<b>(003)</b>				
12210	12848.7724		1	-40
<b>(023)</b>				
220	14157.3123		1	38
322	14225.4924		1	47
<b>(051)</b>				
744	12480.8840		1	80
771	13329.7863		1	-55
845	12685.2532		1	111
881	13865.8493		1	37
880	13865.8493		1	23
937	12641.2467		1	54
10110	13357.1153	1.2	2	23
<b>(061)</b>				
817	13548.1584		1	38
<b>(080)</b>				
937	12667.9783		1	48
1029	13359.0688		1	27
<b>(090)</b>				
505	12832.1188		1	-192
<b>(150)</b>				
431	11733.7897		1	63
845	12601.8038		1	106
946	12807.4902		1	48
963	13425.2693		1	358
<b>(160)</b>				
505	12691.9985		1	286
<b>(221)</b>				
101	13635.1708+		1	-61
111	13651.9814		1	238
221	13757.7727		1	213
322	13826.2276		1	240
331	13919.9622		1	222
413	13884.6231		1	266
515	13922.9622		1	250
717	14166.1557	1	2	240

Note.  $N$  is the number of lines used for the upper energy level determination,  $\sigma$  denotes the corresponding standard deviation calculated for energies determined from more than one transition in 10<sup>-3</sup> cm<sup>-1</sup> units and  $\Delta$  is the deviation of the observed levels from their calculated values in 10<sup>-3</sup> cm<sup>-1</sup>. The level marked by + is in disagreement with that reported in Ref. [7].

energy. Lines such as components of unresolved blends, very weak and saturated ones can have significant errors in their positions and intensities and were then excluded from the energy level derivation.

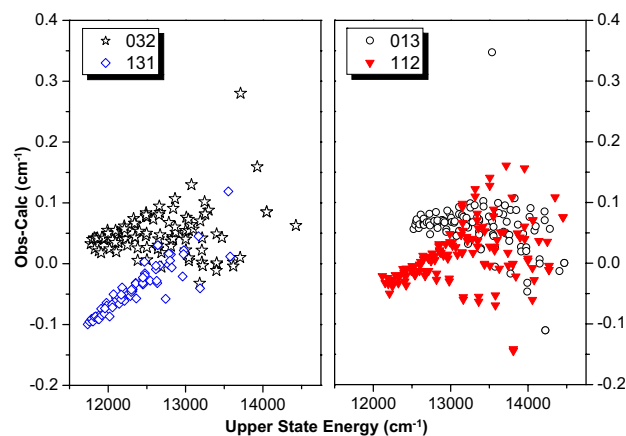


Fig. 4. Difference of the observed and calculated values [19,20] for the energy levels of the (032) and (131) vibrational states (left hand) and (013) and (112) vibrational states (right hand).

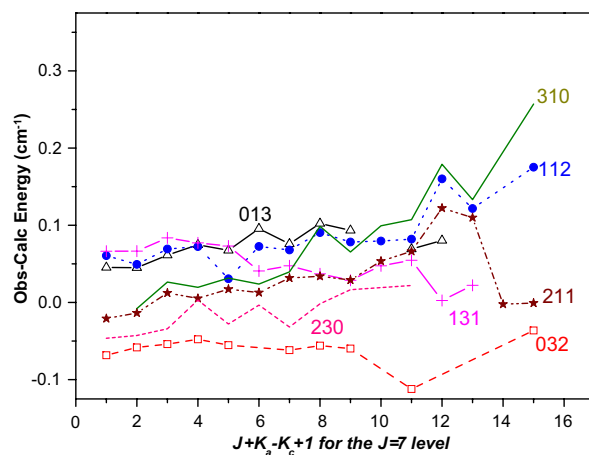


Fig. 5. Difference of the observed and calculated values [19,20] as a function of the quantity  $(J + K_a - K_c + 1)$  for the  $J=7$  energy levels of seven ( $v_1, v_2, v_3$ ) vibrational states which are indicated on the plot. The picture shows a systematic behavior of the (obs-calc) values which confirms the correctness of the assignment.

Table 5  
Energy levels of the (013) and (301) vibrational states of HD<sup>18</sup>O

$JK_aK_c$	$E_{\text{obs}} (\text{cm}^{-1})$	$\sigma$	$N$	$\Delta$
<i>013</i>				
101	11947.8669		1	-275
111	11960.3465		1	-274
110	11963.4779		1	-270
202	11977.7918		1	-275
212	11987.6654	1.2	2	-270
211	11997.0345	0.6	2	-275
221	12034.2836	0.6	2	-263
220	12034.8079		1	-254
303	12021.4542	2	2	-278
313	12028.3240	0.1	2	-273
312	12047.0032		1	-263
322	12079.9039	0.3	2	-266
321	12082.3922	0.1	2	-260
331	12149.4939		1	-247
330	12149.5496		1	-245
404	12077.8014	0.2	2	-276
414	12082.0315	1.2	2	-272
413	12112.8108	2.4	2	-276
423	12140.2983	0.6	2	-267
422	12147.2165		1	-269
432	12211.1231		1	-249
431	12211.4906		1	-251
441	12306.1611		1	-223
440	12306.1781		1	-210
505	12146.1217		1	-276
515	12148.4794	1.2	2	-273
514	12193.6768		1	-282
524	12215.0951	2.2	2	-277
523	12229.5501		1	-301
533	12288.2583		1	-255
542	12383.1043		1	-209
541	12383.1031		1	-251
550	12503.2945		1	-198
606	12226.1949		1	-269
616	12227.4086		1	-278
615	12288.5150		1	-280
625	12303.9000	1.8	2	-274
624	12329.1196		1	-280
633	12384.7966		1	-242
643	12475.6095		1	-249
642	12475.8264		1	-233
660	12739.7016		1	-163
716	12396.1233	0.5	2	-285
726	12406.2501	0.3	2	-277
725	12445.0876		1	-290
735	12488.5281		1	-181
744	12583.8275		1	-246
808	12421.6895		1	-313
818	12422.0186	4.6	2	-278
817	12515.5715		1	-289
827	12521.7392	1.3	2	-276
826	12576.4503		1	-280
836	12611.3738		1	230
835	12628.0996		1	-275
845	12707.6957		1	-241
844	12709.6839		1	-253
909	12537.2998		1	-308
919	12537.4709		1	-272
918	12646.4341		1	-292
928	12650.0989		1	-88
937	12747.6041		1	-288
936	12776.3991		1	-304
10010	12664.8295		1	-311

Table 5 (continued)

$JK_aK_c$	$E_{\text{obs}} (\text{cm}^{-1})$	$\sigma$	$N$	$\Delta$
10110	12664.9153		1	-287
1029	12790.7151		1	-124
11011	12804.2833		1	-313
11111	12804.3259		1	-299
1138	13122.7762		1	-25
12211	13107.8059		1	-787
<i>301</i>				
330	11746.5363		1	-84

Note.  $N$  is the number of lines used for the upper energy level determination,  $\sigma$  denotes the corresponding standard deviation calculated for energies determined from more than one transition in  $10^{-3} \text{ cm}^{-1}$  units and  $\Delta$  is the deviation of the observed levels from their calculated values in  $10^{-3} \text{ cm}^{-1}$ .

Among the 315 levels determined by Bykov et al. [5], 309 are common with ours. However, seventeen of their levels (marked by \* in Tables 2 and 3) deviate by more than  $0.1 \text{ cm}^{-1}$ , some up to a few wavenumbers.

For the levels coinciding within  $10^{-2} \text{ cm}^{-1}$ , the average value of the deviations and the corresponding *rms* are  $-0.4 \times 10^{-3}$  and  $3 \times 10^{-3} \text{ cm}^{-1}$ , respectively. Similarly, we identified in Ref. [7], six levels which have a deviation comprised between 0.1 and  $0.3 \text{ cm}^{-1}$  (they are marked by + in Tables 2 and 3).

Among the valuable information retrieved from the spectra, it is worth noticing that (i) the (032) state is detected for the first time and 64 of its levels could be determined, (ii) 69 levels of the (230) state were assigned in the ICLAS spectrum while only 10 of them were previously determined from Kitt Peak spectra [5], (iii) the band origins of the (230) and (310) could be experimentally determined.

As illustrated in Figs. 2–5, a good agreement is noted between the ICLAS and SP calculated spectra. According to the vibrational state, some systematic tendencies are observed for the deviations of the calculated energy levels from their experimental values (see Figs. 4 and 5), confirming the consistency of our assignments. Maximum values are on the order of  $0.1 \text{ cm}^{-1}$  but the average deviation is only  $0.004 \text{ cm}^{-1}$ .

Table 5 lists the 70 energy levels determined for the HD<sup>18</sup>O isotopologue. The upper level energies were derived by adding the ground state energy values [3] to the observed transitions. Most of them belong to the (013) state which corresponds to the strongest band in this region.

#### 4. Line intensities

In the considered spectral region, HITRAN provides only 164 transitions for H<sub>2</sub><sup>18</sup>O, all lying between 12400 and  $12700 \text{ cm}^{-1}$  and all having line strengths larger than  $7 \times 10^{-26} \text{ cm/molecule}$ , with a maximum intensity of  $4.3 \times 10^{-24} \text{ cm/molecule}$ . The histogram of the ratio of FTS line strengths [7] compared to the results of Schwenke and Partridge calculations [19,20] is shown in Fig. 6. It shows a clear difference on the order of 25% on average,

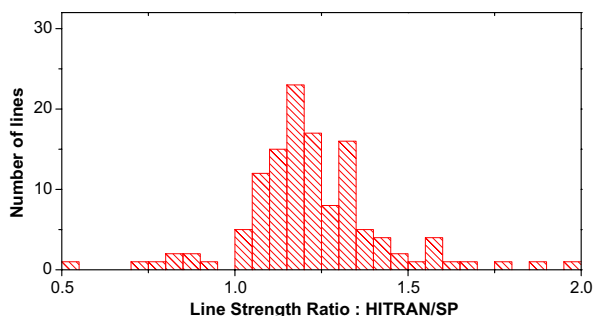


Fig. 6. Histogram of the ratio of the  $\text{H}_2^{18}\text{O}$  line strengths as reported by HITRAN in the  $12400\text{--}12700\text{ cm}^{-1}$  region, by the intensity values calculated by Schwenke and Partridge [19,20].

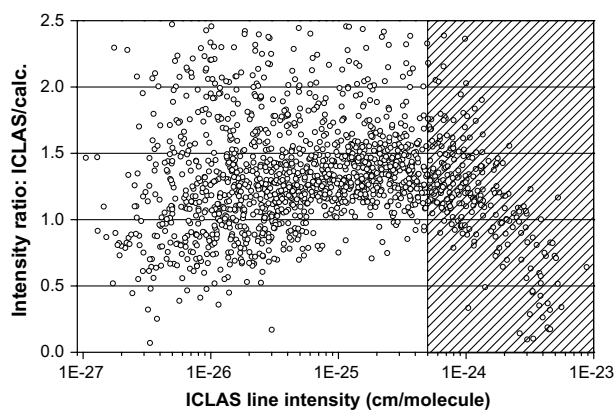


Fig. 7. Ratio of the ICLAS line intensities by calculated [19,20] values versus the ICLAS intensity values. The lines in the hatched region are saturated in the ICLAS spectrum, resulting in an underestimation of their line strength.

the HITRAN values being larger than SP calculations. Note that the line list of Ref. [7] is the one adopted in the last version of the HITRAN database.

As illustrated in Fig. 7, a much more complete comparison (1623 lines) can be performed between the ICLAS line intensities of  $\text{H}_2^{18}\text{O}$  with SP predictions [19,20]. As a consequence of saturation effects in our spectra, only lines with intensities lower than the intensity cutoff fixed at  $5 \times 10^{-25}\text{ cm/molecule}$  have to be considered. The ICLAS/SP intensity ratio falls in the [0.94, 1.56] interval for 61% of the lines and is close to 1.25 in average, which is consistent with the fact that we used  $\text{H}_2^{18}\text{O}$  line intensities provided by HITRAN to determine the isotopic composition of our sample and scale the  $\text{H}_2^{18}\text{O}$  absolute line intensities. The dispersion of the ratio values is not fully satisfactory, in particular for the weakest lines where it reaches a value of 2. This results from a combined effect of the poorer experimental accuracy and a probable worsening of the quality of the intensity predictions.

## 5. Conclusion

The weak absorption spectrum of an  $^{18}\text{O}$  enriched sample of water has been recorded by ICLAS in the region of the sec-

ond decade of vibrational states ( $11\,520\text{--}12\,820\text{ cm}^{-1}$ ). The multiplex advantage of this technique allows for a high data acquisition speed which, combined with a high sensitivity, makes it particularly well suited for the absorption spectroscopy of less abundant isotopologues.

The  $\text{H}_2^{18}\text{O}$  spectrum was assigned on the basis of the high accuracy variational calculations [19,20]. A set of 386 new energy levels belonging to 6 highly excited rovibrational states has been derived. The important set of new energy levels which could be retrieved will be valuable for a further refinement of the potential energy surface of this water isotopologue.

## Acknowledgments

This work is performed in the frame of the European research network QUASAAR (MRTN-CT-2004-512202). It takes part in an effort by a Task Group of the International Union of Pure and Applied Chemistry (IUPAC, Project no. 2004-035-1-100) to compile, determine, and validate, both experimentally and theoretically, accurate frequency, energy level, line intensity, line width, and pressure effect spectral parameters of all major isotopologues of water. AC (Grenoble) is grateful for the financial support provided by Programme National LEFE (CHAT). O. V. Naumenko (IAO, Tomsk) is acknowledged for providing us the line list attached to Ref. [5].

## Appendix A. Supplementary data

Supplementary data for this article are available on ScienceDirect ([www.sciencedirect.com](http://www.sciencedirect.com)) and as part of the Ohio State University Molecular Spectroscopy Archives ([http://msa.lib.ohio-state.edu/jmsa\\_hp.htm](http://msa.lib.ohio-state.edu/jmsa_hp.htm)).

## References

- [1] L.S. Rothman, D. Jacquemart, A. Barbe, D. Chris Benner, M. Birk, L.R. Brown, M.R. Carleer, C. Chackerian Jr., K. Chance, V. Dana, V.M. Devi, J.-M. Flaud, R.R. Gamache, A. Goldman, J.-M. Hartmann, K.W. Jucks, A.G. Maki, J.Y. Mandin, S.T. Massie, J. Orphal, A. Perrin, C.P. Rinsland, M.A.H. Smith, J. Tennyson, R.N. Tolchenov, R.A. Toth, J. VanderAuwera, P. Varanasi, G. Wagner, J. Quant. Spectrosc. Radiat. Transfer 96 (2005) 139–204.
- [2] J.-P. Chevillard, J.-Y. Mandin, J.-M. Flaud, C. Camy-Peyret, Can. J. Phys. 63 (1985) 1112–1127.
- [3] J.-P. Chevillard, J.-Y. Mandin, J.-M. Flaud, C. Camy-Peyret, Can. J. Phys. 64 (1986) 746–761.
- [4] J.-P. Chevillard, J.-Y. Mandin, J.-M. Flaud, C. Camy-Peyret, Can. J. Phys. 65 (1987) 777–789.
- [5] A.D. Bykov, O.V. Naumenko, T. Petrova, A. Scherbakov, L.N. Sinitsa, J.-Y. Mandin, C. Camy-Peyret, J.-M. Flaud, J. Mol. Spectrosc. 172 (1995) 243–253.
- [6] M. Tanaka, J.W. Brault, J. Tennyson, J. Mol. Spectrosc. 216 (2002) 77–80.
- [7] M. Tanaka, O.V. Naumenko, J.W. Brault, J. Tennyson, J. Mol. Spectrosc. 234 (2005) 1–950.
- [8] M. Tanaka, M. Snee, W. Ubachs, J. Tennyson, J. Mol. Spectrosc. 226 (2004) 1–6.
- [9] M. Herman, J. Liévin, J. Vander Auwera, A. Campargue, Adv. Chem. Phys. 108 (1999) 1–431.

- [10] A. Campargue, I. Vasilenko, O. Naumenko, *J. Mol. Spectrosc.* 234 (2005) 216–227.
- [11] Shui-Ming Hu, O.N. Ulenikov, E.S. Bekhtereva, G.A. Onopenko, Sheng-Gui He, Hai Lin, Ji-Xin Cheng, Qing-Shi Zhu, *J. Mol. Spectrosc.* 212 (2002) 89–95.
- [12] S. Hu, H. Lin, S. He, J. Cheng, Q. Zhu, *Phys. Chem. Chem. Phys.* 1 (1999) 3727–3730.
- [13] F. Mazzotti, O.V. Naumenko, S. Kassi, A.D. Bykov, A. Campargue, *J. Mol. Spectrosc.* 239 (2006) 174–181.
- [14] R. Schermaul, R.C.M. Learner, D.A. Newnham, J. Ballard, N.F. Zobov, D. Belmiloud, J. Tennyson, *J. Mol. Spectrosc.* 208 (2001) 43–50.
- [15] R. Schermaul, R.C.M. Learner, A.A.D. Canas, J.W. Brault, O.L. Polyansky, D. Belmiloud, N.F. Zobov, J. Tennyson, *J. Mol. Spectrosc.* 211 (2002) 169–178.
- [16] R.N. Tolchenov, J. Tennyson, J.W. Brault, A.A.D. Canas, R. Schermaul, *J. Mol. Spectrosc.* 215 (2002) 269–274.
- [17] A. Kachanov, A. Charvat, F. Stoeckel, *J. Opt. Soc. Am. B.* 11 (1994) 2412–2421.
- [18] A. Campargue, M. Chenevier, F. Stoeckel, *Spectrochim. Acta Rev.* 13 (1990) 69–88.
- [19] H. Partridge, D.W. Schwenke, *J. Chem. Phys.* 106 (1997) 4618–4639.
- [20] D.W. Schwenke, H. Partridge, *J. Chem. Phys.* 113 (2000) 6592–6597.
- [21] R.A. Toth, *J. Opt. Soc. Am. B* 9 (1992) 462–482.